Research Square

Preprints are preliminary reports that have not undergone peer review.
They should not be considered conclusive, used to inform clinical practice,
or referenced by the media as validated information.

# ALKBH5-mediated m6A demethylation of SLC12A8 gene promotes EMT and TAM resistance in breast cancer

**Dongmin Yu**

183709555680163.com

First Affiliated Hospital of Gannan Medical

**Yan Meng**

Tumor Hospital of Guangxi Medical University

**Haiyang Guan**

Gannan Medical University

**Yongzhen Li**

Gannan Medical University

**Haiyan Wang**

Gannan Medical University

**Yao Zhou**

First Affiliated Hospital of Gannan Medical

**Rongzhen xie**

First Affiliated Hospital of Gannan Medical

**Research Article**

**Keywords:** SLC12A8, ALKBH5, m6A modification, tamoxifen resistance

**Posted Date:** November 23rd, 2026

**DOI:** https://doi.org/10.21203/rs.3.rs-11571856/v1

**License:** This work is licensed under a Creative Commons Attribution 4.0 International License.
Read Full License

**Additional Declarations:** No competing interests reported.

# ALKBH5-mediated m6A demethylation of SLC12A8 gene promotes EMT and TAM resistance in breast cancer

Dongmin Yu[a,†,*], Yan Meng[c,*], Haiyang Guan[b,*], Yongzhen Li[b]， Haiyan Wang[b],Yao Zhou,[d,†] and Rongzhen xie[e,†]

[a] Department of Breast Disease Comprehensive Center, First Affiliated Hospital of Gannan Medical University, Ganzhou, 341000, China.

[b] First Clinical Medical College of Gannan Medical University , Ganzhou, 341000, China.

[c]Department of Breast, Bone&Soft Tissue Oncology, Guangxi Medical University Cancer Hospital, 530021,Nanning,China,

[d] Nanchang Medical College,Nanchang Peoples Hospital, Department Breast Surgery, Nanchang 330006,China.

[e] Department of General Surgery, The First Affiliated Hospital of Gannan Medical University, Ganzhou, Jiangxi Province, China, 341000, China.

Corresponding Author:

Dongmin Yu,Department of Breast Disease Comprehensive Center, First Affiliated Hospital of Gannan Medical University, Ganzhou, 341000, China. 18370955568@163.com;

Rongzhen xie,Department of General Surgery , The First Affiliated Hospital of Gannan Medical University, Ganzhou, Jiangxi Province, China, 341000, China. yfyxierongzhen@163.com.

Yao Zhou,Nanchang Medical College,Nanchang Peoples Hospital, Department Breast Surgery, Nanchang 330006,China. zhouyaoican@163.com

These authors contributed equally to this work.

**Abstract:**

Background:The role and post-transcriptional regulatory mechanisms of SLC12A8 in breast cancer remain unclear. This study explores its clinical relevance, biological functions, and m6A regulatory mechanisms.Methods:TCGA, GTEx, and Kaplan–Meier Plotter were utilized

to analyze SLC12A8 expression and prognosis; a xenograft tumor model was used to evaluate tumor growth; SRAMP and RM2Target were employed to predict m6A modifications, which were verified by MeRIP-qPCR and RIP; actinomycin D assay, Co-IP, and Western blot were used to examine the ALKBH5–SLC12A8 axis; functional experiments were conducted combining CCK-8, EdU, flow cytometry, and Transwell assays; GDSC2 and GSVA were used to analyze drug sensitivity and pathway enrichment.Results:SLC12A8 was significantly highly expressed in breast tumors ($P < 0.0001$), and high expression was associated with worse OS, RFS, and DMFS in breast cancer ($P < 0.01$). Overexpression of SLC12A8 promoted xenograft tumor growth and malignancy, accompanied by elevated SLC12A8 protein expression. SRAMP predicted 23 m6A sites in SLC12A8, including 9 with high or very high confidence, with GGACU being a high-confidence site; MeRIP-qPCR and RIP confirmed that SLC12A8 was enriched by the m6A antibody, with the highest enrichment by ALKBH5. Silencing ALKBH5 increased SLC12A8 m6A enrichment and decreased its stability, while overexpressing ALKBH5 reduced m6A enrichment and elevated SLC12A8 protein; Co-IP confirmed their interaction. Functionally, silencing SLC12A8 inhibited breast cancer cell viability, proliferation, migration, and invasion, and promoted apoptosis, which could be reversed by ALKBH5 overexpression, while silencing ALKBH5 reversed the effects of SLC12A8 overexpression. GDSC2 showed that the tamoxifen IC50 was significantly higher in the high SLC12A8 expression group ($P < 0.0001$); GSVA suggested the PI3K/AKT/mTOR pathway was most closely related, and Western blot confirmed that silencing ALKBH5 inhibited p-AKT/mTOR expression. Conclusion:SLC12A8 is highly expressed in breast cancer, indicating a poor prognosis for breast cancer patients, and promotes tumor growth and tamoxifen resistance. ALKBH5-mediated m6A demethylation stabilizes SLC12A8. The ALKBH5–SLC12A8 axis regulates breast cancer progression via

the PI3K/AKT/mTOR pathway and may serve as a potential prognostic biomarker and therapeutic target.

**Keywords:** SLC12A8; ALKBH5; m6A modification; tamoxifen resistance

## 1.Introduction

Breast cancer is a major threat to global women's health, and its high mortality is closely linked to tumor metastasis and therapy resistance. Tamoxifen, as the cornerstone drug for endocrine therapy of hormone receptor-positive (HR+) breast cancer, sees resistance emerge as the primary cause of clinical treatment failure. The mechanisms of resistance are complex, involving multiple factors such as alterations in the estrogen receptor α signaling pathway, activation of compensatory growth factor pathways, increased tumor heterogeneity, and remodeling of the tumor microenvironment. In recent years, epithelial-mesenchymal transition (EMT), as a key biological process promoting tumor invasion, metastasis, and acquisition of therapy resistance, has played an increasingly prominent role in breast cancer resistance research. Studies indicate that EMT not only endows tumor cells with stronger migration and invasion capabilities but also participates in the formation of endocrine resistance through mechanisms regulating cell stemness, cell cycle, and apoptosis resistance. However, the specific molecular mechanisms by which it regulates endocrine resistance, particularly its interaction with RNA epigenetic modifications, remain unclear.

N6-methyladenosine (m6A) modification is the most common epigenetic modification in eukaryotic mRNA, dynamically and reversibly regulating all aspects of mRNA metabolism. ALKBH5, as an important m6A demethylase, affects the biological behavior of tumors by regulating the m6A modification levels of target gene RNAs. Recent studies have shown that the expression of ALKBH5 in HR+ breast cancer is closely related to the response to

endocrine therapy, but its specific mechanism of action still requires in-depth exploration. Solute carrier family 12 member 8 (SLC12A8) is an electroneutral cation-coupled transporter protein primarily involved in cell volume regulation and osmotic pressure balance. Studies have confirmed that SLC12A8 is abnormally expressed in various tumors and is closely related to tumor metabolic reprogramming. Notably, multiple conserved m6A modification sites exist in the coding sequence of SLC12A8, suggesting it may be finely regulated by m6A modifications, but its specific regulatory mechanisms, especially its association with RNA modifications, remain to be elucidated.

This study comprehensively utilizes multi-omics analysis, molecular biology, cellular functional experiments, and in vivo mouse models to deeply explore how ALKBH5 affects the translation efficiency of SLC12A8 by regulating its m6A modification levels. It aims to reveal the novel functions of m6A modification in breast cancer endocrine resistance, providing brand-new combined therapeutic targets and a theoretical basis for overcoming TAM-related resistance in breast cancer.

## 2.Materials and methods

### 2.1Bioinformatics analysis

The transcriptome data and corresponding clinical information in this study were downloaded from the UCSC XENA database. Breast cancer tissue transcriptome data were sourced from the TCGA database, and normal breast tissue transcriptome data integrated the TCGA and GTEx databases. The GEPIA platform was used to analyze the expression distribution of SLC12A8 in breast tumor and normal breast tissue samples[1]. The Kaplan-Meier Plotter database was used to analyze the association between SLC12A8 gene expression and the prognosis of breast cancer patients[2]. Evaluation metrics included overall survival (OS),

relapse-free survival (RFS), and distant metastasis-free survival (DMFS). The log-rank test was used for statistical comparison of the survival curves.

The SRAMP online tool was used to predict the m6A modification sites of SLC12A8 and to screen for high-confidence modification sites[3]. The RM2Target database was utilized to predict potential m6A modification-related regulatory molecules for SLC12A8, and to analyze the correlation between SLC12A8 expression levels and its methylation modification levels. Drug sensitivity analysis was conducted based on the GDSC2 database to explore the relationship between SLC12A8 expression and the half-maximal inhibitory concentration (IC50) of tamoxifen (TAM)[4]. The difference in TAM-IC50 between high and low SLC12A8 expression groups was compared, and Spearman rank correlation was used for correlation evaluation. The HALLMARK pathway dataset from the MsigDB database was retrieved to conduct Gene Set Variation Analysis (GSVA), calculate pathway activity scores for each sample, analyze the correlation between SLC12A8 expression levels and pathway scores, and screen for potential downstream signaling pathways.

**2.2 Cell lines and cell culture**

The cells used in this experiment included human breast cancer cell lines MDA-MB-231, MCF-7, SK-BR-3, and human normal mammary epithelial cells Hs 578Bst purchased from the Institute of Biochemistry and Cell Biology, Chinese Academy of Sciences (Shanghai, China). Our laboratory constructed the tamoxifen-resistant cell line MCF-7/TAM using a concentration gradient escalation induction method. MCF-7 cells were cultured in DMEM high-glucose medium supplemented with 10% fetal bovine serum; MDA-MB-231 and Hs 578Bst cells were cultured in DMEM/F12 medium containing 10% fetal bovine serum. SK-BR-3 cells were cultured in McCoy's 5A medium containing 10% fetal bovine serum. MCF-7/TAM resistant cells were maintained in complete medium containing 1 μmol/L tamoxifen. All cells were incubated in a constant temperature incubator at 37 °C with 5% $CO_2$ and

saturated humidity. Cells in the logarithmic growth phase were selected for experiments, and all cells were tested negative for mycoplasma.

**2.3 Plasmid construction and cell transfection**

SLC12A8 shRNA lentiviral vectors, ALKBH5 overexpression plasmids, and short hairpin RNAs (shRNAs) targeting SLC12A8 and ALKBH5 were constructed and synthesized by Shanghai Sangon Biotech. Transient transfection was performed according to the instructions of the Lipofectamine 3000 reagent.

**2.4 RNA extraction and quantitative real-time PCR (qRT-PCR)**

Total RNA from cells was extracted using TRIzol reagent, and RNA concentration and purity were measured using a NanoDrop2000 instrument. 1 μg of total RNA was taken to synthesize cDNA using the HiScript III RT SuperMix reverse transcription kit. The qRT-PCR reaction was performed using ChamQ Universal SYBR qPCR Master Mix, with GAPDH as the internal reference gene, and amplification was completed on a LightCycler 480 II instrument. The $2^{-\Delta\Delta Ct}$method was used to calculate the relative gene expression. The primer sequences are as follows:

SLC12A8

Forward, 5’-TGGCGTCTACTCCATGATCTCC-3’, and Reverse, 5’-CCGAGATGGATTCAGCAAAGCC-3’;

GAPDH

Forward, 5’ -TAGATGACACCCGTCCCTGA-3’, and Reverse, 5’-ACCTCCACCTGTCCTTAGTG -3’.

ALKBH5

Forward,5'-ATTCTAGAGCTAGCGAAATTCATG GCCGGCCGACGCG GC-3',and Reverse, 5'-ATCCTTCGCGGCCGCGGATCCTCAGTGCGGCCGCAT CTTACC-3'.

GAPDH

Forward：TGCACCACCAACTGCTTAGC, and Reverse：AGGGCTTGG GGCAAATTGTT.

**2.5 Western blot**

Total cell protein was extracted using RIPA lysis buffer supplemented with 1% PMSF and phosphatase inhibitors, and protein sample concentration was determined by the BCA method. Equal amounts of protein were separated by SDS-PAGE and wet-transferred onto PVDF membranes; they were blocked with 5% skim milk at room temperature for 1 h. Primary antibodies were added and incubated overnight at 4 °C. The primary antibodies used included ALKBH5, SLC12A8, AKT, p-AKT, mTOR, p-mTOR, and GAPDH. Membranes were washed 3 times with TBST for 10 min each, then incubated with HRP-labeled secondary antibodies at room temperature for 1 h, and washed 3 times with TBST for 10 min each. After washing, ECL chemiluminescent substrate was used for development and imaging, and ImageJ software was used for semi-quantitative analysis of protein band gray values.

**2.6 Co-immunoprecipitation (Co-IP)**

Cells were collected and total protein was extracted. 500 μg of total protein was taken, corresponding antibodies and Protein A/G magnetic beads were added, and incubated with rotation overnight at 4 °C. The magnetic beads were washed 5 times with pre-chilled washing buffer, 2×SDS loading buffer was added, and the samples were boiled for denaturation. The eluted products were subjected to Western blot analysis to verify the binding relationships between proteins.

**2.7 Actinomycin D mRNA stability assay**

Cells were seeded into 6-well plates, and when cell confluence reached 70%, actinomycin D was added at a final concentration of 5 μg/mL. Cells were collected and total RNA was extracted at 0, 2, 4, 6, and 8 h, respectively. The relative amount of SLC12A8 mRNA at different time points was detected by qRT-PCR to evaluate mRNA stability.

### 2.8 RNA immunoprecipitation (RIP)

The experiment was conducted according to the EZ-Magna RIP kit instructions. Cells were lysed, and the cell lysate was incubated with magnetic beads conjugated to IgG control antibody, m6A antibody, and ALKBH5 antibody, respectively, at 4 °C overnight. After thoroughly washing the magnetic beads, the bound RNA was purified via proteinase K digestion. qRT-PCR was used to detect the RNA enrichment level of SLC12A8, and the relative enrichment fold was calculated using the IgG group as a control.

### 2.9 MeRIP-qPCR

Total cellular RNA was extracted and fragmented. An m6A methylated RNA immunoprecipitation kit was used to perform immunoprecipitation with an m6A antibody and an IgG control antibody, respectively. The enriched RNA was eluted and purified, and qRT-PCR was used to detect the level of SLC12A8 in the precipitated products to assess the m6A modification enrichment of SLC12A8.

### 2.10 CCK-8 cell viability assay

Cells were seeded into 96-well plates at a density of $3\times10^3$ cells/well, with 5 replicate wells per group. At 0, 24, 48, 72, and 96 h time points, 10 μL of CCK-8 reagent was added to each well, incubated at 37 °C for 2 h, and the absorbance at 450 nm was measured by a microplate reader. This experiment was independently repeated at least 3 times.

### 2.11 EdU cell proliferation assay

The procedure was performed according to the EdU cell proliferation assay kit instructions. Cells were seeded into 96-well plates and incubated with EdU working solution for 2 h; after cell fixation and permeabilization, fluorescent click chemistry was performed, and nuclei were counterstained with Hoechst 33342. Images were acquired using a fluorescence microscope, and ImageJ software was used to calculate the ratio of EdU-positive cells to total cells. The experiment was independently repeated 3 times.

### 2.12 Flow cytometry analysis of apoptosis

Cells from each treatment group were collected, and cell staining was performed according to the Annexin V-FITC apoptosis detection kit instructions. Flow cytometry was used for detection to analyze the proportion of apoptotic cells. The experiment was independently repeated 3 times.

### 2.13 Wound healing assay

Cells were seeded into 6-well plates and cultured until they completely covered the bottom of the well. A 200 μL sterile pipette tip was used to make a linear scratch, PBS was used to wash off suspended and detached cells, and serum-free medium was replaced. Images were acquired under an inverted microscope at 0 h and 24 h, respectively. ImageJ software was used to analyze the wound healing area and calculate cell migration capacity. The experiment was independently repeated 3 times.

### 2.14 Transwell migration and invasion assays

Migration assay: $2\times10^4$ cells were resuspended in serum-free medium and added to the upper Transwell chamber. Complete medium containing 20% fetal bovine serum was added to the lower chamber as a chemotactic stimulus, and incubated at 37 °C for 24 h. For the invasion assay, Matrigel matrix gel was pre-coated in the upper chamber, and the rest of the procedure was identical to the migration assay. After incubation, non-invading cells on the upper surface of the membrane were removed, fixed with 4% paraformaldehyde, and stained with crystal violet. Five random fields of view were selected under the microscope to count the number of cells that passed through the membrane. The experiment was independently repeated 3 times.

### 2.15 Immunohistochemical staining (IHC)

Breast cancer and paired normal breast tissues were fixed in 4% neutral formalin, paraffin-embedded, and sectioned at 4 μm. After dewaxing and hydration, the sections underwent high-pressure antigen retrieval in sodium citrate buffer; 3% hydrogen peroxide was used to

block endogenous peroxidase, and goat serum was used to block non-specific binding sites. SLC12A8 primary antibody was applied and incubated overnight at 4 °C; secondary antibody was subsequently incubated, developed with DAB, and counterstained with hematoxylin. After graded dehydration, the slides were mounted. The H-score scoring system was used to evaluate the staining level of the tissue sections.

## 3.Statistical analysis

All experimental data are expressed as mean ± standard deviation (mean ± SD). Statistical analysis was performed using R software (version 4.2.1) and GraphPad Prism (version 10). Comparisons between two groups were made using a two-tailed Student's t-test; comparisons among multiple groups were made using one-way analysis of variance (ANOVA), followed by Tukey's multiple comparison test. Correlation analysis was performed using Pearson or Spearman correlation analysis. Survival analysis was performed using the Kaplan-Meier method, and survival curve differences were compared using the log-rank test. Comparisons of IC50 between groups were made using the Mann-Whitney U test. A P value $< 0.05$ was considered statistically significant.

# 4. Results

### 4.1 Expression differences of SLC12A8 among different breast cancer and normal tissues and its correlation with prognosis

In this project, TCGA and GTEx data were both downloaded from the UCSC XENA database. Breast cancer tissue analysis data were from the TCGA database, and normal tissue data were sourced from the TCGA and GTEx databases. Data obtained from the GEPIA website was used to analyze SLC12A8. (Fig. 1A) shows the expression distribution of SLC12A8 in tumors and normal samples in the human body map; (Fig. 1B-C) shows the comparison of SLC12A8 expression between normal tissues and breast tumor tissues.

Compared with the normal group, SLC12A8 expression was significantly elevated in breast tumor tissues ($P < 0.0001$); (Fig. 1D) shows immunohistochemistry images of normal (left) and tumor (right) tissues, where SLC12A8 protein expression was significantly increased in breast tumors. The Kaplan-Meier Plotter database was utilized to analyze the association between SLC12A8 gene expression and the prognosis of breast cancer patients. Compared with the control group, the survival-related metrics OS, RFS, and DMFS of the high SLC12A8 expression group were all significantly lower than those of the low expression group ($P < 0.01$) (Fig. 1E). This indicates that the expression of the SLC12A8 gene is closely related to the prognosis of breast cancer patients, and patients with high SLC12A8 expression have a worse prognosis.

As shown in Figure 1, SLC12A8 is overexpressed in breast cancer and correlates with poor clinical prognosis.

Figure 1. Expression profile and prognostic significance of SLC12A8 in breast cancer.

Comparison of SLC12A8 expression between normal and breast tumour tissues from TCGA-GTEx datasets. Immunohistochemical staining validates elevated SLC12A8 protein in breast tumour specimens. Kaplan-Meier survival curves demonstrate that high SLC12A8 expression predicts unfavourable OS, RFS and DMFS in breast cancer patients.

**4.2 SLC12A8 promotes tumor growth**

The study constructed an SLC12A8 overexpression xenograft tumor model in mice using lentivirus. WB detected SLC12A8 expression in the tumor tissues of mice in each group, and the results showed that compared with the LV-NC group, SLC12A8 expression in the LV-SLC12A8 group was significantly upregulated, confirming the efficacy of the overexpression (Fig. 2A). As shown in Fig. 2B, compared with the negative control LV-NC group, both the volume and weight of xenograft tumors in the SLC12A8 overexpression group (LV-SLC12A8) were significantly increased. HE staining of tumor tissues indicated that SLC12A8

significantly enhanced the malignancy of tumor tissues (Fig. 2C). Immunohistochemistry results showed that SLC12A8 protein expression was significantly increased in the LV-SLC12A8 group (Fig. 2D).

The in-vivo tumour-promoting effect of SLC12A8 is presented in Figure 2.

Figure 2. SLC12A8 accelerates xenograft tumour growth in vivo.

Lentivirus-mediated SLC12A8 overexpression was confirmed by western blot. Tumour volume and weight were increased in the LV-SLC12A8 group. HE staining shows higher malignant features in overexpressing tumours. IHC staining confirms higher SLC12A8 protein level in xenograft tissues.

**4.3 Analysis of SLC12A8 m6A modification sites**

The SRAMP website was used to analyze the m6A modification sites of SLC12A8, and a total of 23 modification sites were obtained, including 9 with high or very high confidence (Fig. 3B). Among them, GGACU was a high-confidence site (Fig. 3B). Subsequently, the m6A modification database website RM2Target was used to analyze the modification targets of different methyltransferases, predicting that SLC12A8 activity might be modified by ALKBH5 and FTO. It also showed the correlation between SLC12A8 and methylation: the higher the SLC12A8 expression, the lower its methylation modification (Fig. 3C). MeRIP-qPCR experiments verified that SLC12A8 was significantly enriched in the m6A antibody (Fig. 3D); RIP experiments detected that SLC12A8 could be significantly enriched with m6A-related proteins, among which ALKBH5 showed the highest enrichment (Fig. 3E).

$m^6A$ modification sites prediction and experimental validation for SLC12A8 are summarised in Figure 3.

Figure 3. Prediction and verification of $m^6A$ modification sites on SLC12A8 mRNA.

SRAMP predicts multiple high-confidence $m^6A$ sites within SLC12A8 sequence. RM2Target database suggests ALKBH5 as a potential regulator. MeRIP-qPCR confirms $m^6A$

modification of SLC12A8, and RIP assay verifies the enrichment of SLC12A8 by ALKBH5 protein.

**4.4 ALKBH5 mediates SLC12A8 m6A modification**

MeRIP-qPCR was used to analyze the effect of silencing and overexpressing ALKBH5 on the m6A modification level of SLC12A8. The results showed that when ALKBH5 was silenced, the amount of SLC12A8 enriched on the m6A antibody increased (Fig. 4A); conversely, after overexpressing ALKBH5, the amount of SLC12A8 enriched on the m6A antibody decreased (Fig. 4B). In summary, ALKBH5 is involved in the m6A modification of SLC12A8. Actinomycin D assay to detect SLC12A8 stability revealed that silencing ALKBH5 reduced SLC12A8 stability (Fig. 4C). Co-IP experiments verified that ALKBH5 and SLC12A8 could interact (Fig. 4D); detection showed that SLC12A8 expression increased after ALKBH5 overexpression (Fig. 4E).

ALKBH5-mediated $m^6A$ demethylation and stabilisation of SLC12A8 are shown in Figure 4.

Figure 4. ALKBH5 mediates $m^6A$ demethylation and stabilises SLC12A8 mRNA.

MeRIP-qPCR shows that ALKBH5 silencing increases, whereas ALKBH5 overexpression reduces $m^6A$ enrichment of SLC12A8. Actinomycin D assay demonstrates that ALKBH5 knockdown shortens SLC12A8 mRNA half-life. Co-IP validates protein interaction between ALKBH5 and SLC12A8. Western blot detects SLC12A8 protein changes upon ALKBH5 manipulation.

**4.5 ALKBH5 mediates the regulation of breast cancer cells by SLC12A8**

qRT-PCR was used to detect the expression of ALKBH5 in breast cancer cell lines MDA-MB-231, MCF-7, SK-BR-3, and normal breast cell line Hs 578Bst. The results showed that compared with Hs 578Bst cells, ALKBH5 expression was significantly upregulated in MDA-MB-231, MCF-7, and SK-BR-3 (Fig. 5A). qRT-PCR was used to detect SLC12A8 expression levels in each group of cells. The results showed that after silencing SLC12A8, SLC12A8

expression level decreased, and after overexpressing ALKBH5, SLC12A8 expression was upregulated (Fig. 5B). CCK-8 was used to detect cell viability. As shown in Fig. 5C, silencing SLC12A8 inhibited the viability of breast cancer cells, which was reversed by overexpressing ALKBH5. EdU was used to detect cell proliferation capacity (Fig. 5D); silencing ALKBH5 reversed the promoting effect of SLC12A8 overexpression on the proliferation of breast cancer cells. In addition, flow cytometry was used to detect the apoptosis level (Fig. 5E), and the results showed that silencing ALKBH5 significantly promoted the apoptosis of breast cancer cells.

Cell functional changes regulated by the ALKBH5-SLC12A8 axis are displayed in Figure 5.

Figure 5. ALKBH5 participates in SLC12A8-driven cell proliferation and apoptosis of breast cancer cells.

ALKBH5 mRNA expression in breast cancer cell lines and normal mammary epithelial cells. qRT-PCR detects SLC12A8 expression under different genetic manipulations. CCK-8 and EdU assays evaluate cell viability and proliferation. Flow cytometry analyses cell apoptosis under SLC12A8 and ALKBH5 alteration.

**4.6 Effect of ALKBH5-mediated SLC12A8 on the invasion capacity of breast cancer cells**

Wound healing assay and Transwell assay (Fig. 6A, B) showed that over-expression of SLC12A8 promoted the migration and invasion of breast cancer cells, and this phenomenonwas reversed after silencing ALKBH5.

Cell migration and invasion phenotypes are illustrated in Figure 6.

Figure 6. ALKBH5-SLC12A8 axis modulates migration and invasion capacity of breast cancer cells.

Wound-healing and Transwell assays show that SLC12A8 overexpression promotes breast cancer cell migration and invasion, and these malignant phenotypes are abrogated by ALKBH5 silencing.

### 4.7 ALKBH5-mediated SLC12A8 effect on breast cancer TAM resistance

Data from GDSC2 was used to analyze the relationship between gene expression and drug IC50 (https://www.cancerrxgene.org/), and plots were generated for the IC50 differences of each drug between high and low gene expression groups, as well as the correlation between gene expression and IC50 (spearman). The results showed that SLC12A8 gene expression was closely related to the IC50 of endocrine therapy drugs for ER-positive breast cancer (Fig. 7A); compared with the control group, the IC50 of the endocrine therapy drug ER modulator (Tamoxifen, TAM) in the high SLC12A8 expression group was significantly higher than that in the low expression group ($P < 0.0001$).EdU was used to detect cell proliferation capacity (Fig. 7B); silencing ALKBH5 reversed the promoting effect of SLC12A8 overexpression on the proliferation of breast cancer cells.In addition, Transwell assay (Fig. 7C) showed that overexpression of SLC12A8 promoted the migration and invasion of breast cancer cells, and this phenomenon was reversed after silencing ALKBH5.

The role of ALKBH5-SLC12A8 in tamoxifen resistance is shown in Figure 7.

Figure 7. SLC12A8 confers tamoxifen resistance regulated by ALKBH5.

GDSC2 drug-sensitivity analysis reveals higher tamoxifen IC50 in SLC12A8-high group. EdU and Transwell assays demonstrate that ALKBH5 knockdown rescues the pro-proliferative and pro-migratory effects induced by SLC12A8 overexpression in tamoxifen-resistant cells.

### 4.8 Screening of potential downstream pathways of SLC12A8 in breast cancer TAM resistance

The Oncomine database showed that m6A-related enzymes, including ALKBH5, METTL3, METTL14, WTAP, and FTO, were differentially expressed between breast cancer and normal tissues (Fig. 8A). Using the latest updated MsigDB database HALLMARK pathway dataset, which includes 50 hallmark pathways. First, GSVA scoring was performed to calculate the correlation between SLC12A8 gene expression and pathway scores, and a correlation plot was generated. As shown in the figure below, SLC12A8 had the closest relationship with the PI3K/AKT/mTOR signaling pathway (Fig. 8B). The effect of ALKBH5 knockdown on the PI3K/AKT/mTOR pathway was then verified. WB was used to detect the expression levels of PI3K/AKT/mTOR pathway-related proteins in MCF-7/TAM cells (Fig. 8C), and the results showed that silencing ALKBH5 decreased the expression levels of SLC12A8, ALKBH5, p-AKT (Ser473), and p-mTOR (Ser2448).

Downstream signalling pathway screening and validation are presented in Figure 8.

Figure 8. Identification of PI3K/AKT/mTOR as downstream pathway of the ALKBH5-SLC12A8 axis.

Differential expression of m$^6$A-related enzymes in breast cancer. GSVA analysis identifies PI3K/AKT/mTOR as the most correlated pathway with SLC12A8. Western blot detects alterations of PI3K/AKT/mTOR-related phosphorylated proteins upon ALKBH5 knockdown in MCF-7/TAM cells.

## 5. Discussion

Members of the solute carrier (SLC) family play important roles in tumor metabolic reprogramming and drug transport. SLC12A8, identified as a nicotinamide mononucleotide (NMN) transporter[5], can affect the energy homeostasis of tumor cells by regulating NAD+ metabolism[6]; it is upregulated in most tumor types and predicts poor survival outcomes[7].

This study, based on the integrated analysis of multiple databases including TCGA and GTEx, combined with immunohistochemical validation, confirmed that SLC12A8 is significantly highly expressed in breast tumor tissues, and its high expression is closely related to the poor prognosis (OS, RFS, DMFS) of breast cancer patients. This finding is consistent with previous research results; Li et al. [8] reported that SLC12A8 promotes the proliferation and invasion of breast cancer cells by activating the TLR/NLR signaling pathway, while the study by Kim et al. [9] found from a pharmacogenomics perspective that single nucleotide polymorphisms of SLC12A8 are significantly associated with survival after breast cancer chemotherapy. This study further expands the above understanding, specifying the clinical significance of SLC12A8 from a pan-cancer prognostic biomarker to the scenario of TAM resistance in ER-positive breast cancer.

Endocrine therapy resistance is a core challenge in the clinical management of ER-positive breast cancer[10,11]. This study, based on GDSC2 database analysis, showed that high SLC12A8 expression is significantly associated with an increased IC50 of TAM, and overexpression of SLC12A8 promotes the proliferation, migration, and invasion of TAM-resistant cells. This finding elevates SLC12A8 from a mere prognostic biomarker to a potential therapeutic target. The pan-cancer analysis by Yu et al. has already proposed the possibility of SLC12A8 as an immunotherapy target, and this study further suggests that targeted inhibition of SLC12A8 may simultaneously have the potential to overcome endocrine resistance. Interestingly, the effects of SLC12A8 overexpression on the proliferation and migration/invasion capacities of breast cancer cells were reversed in the absence of ALKBH5. CCK-8 and EdU experiments showed that silencing ALKBH5 reversed the promotion of proliferation caused by SLC12A8 overexpression, while Transwell assays showed that silencing ALKBH5 reversed the promoting effect of SLC12A8 on migration and invasion.

ALKBH5, as one of the two known human m6A demethylases, plays a crucial role in the epitranscriptomics of m6A-modified RNA. Through SRAMP prediction combined with MeRIP-qPCR validation, we found that SLC12A8 mRNA contains modification sites that can be significantly enriched by the m6A antibody; silencing ALKBH5 led to increased m6A modification levels and decreased mRNA stability of SLC12A8, whereas overexpressing ALKBH5 produced the opposite effect; Co-IP experiments further confirmed the physical interaction between the two. This regulatory pattern is highly consistent with the functional characteristics of ALKBH5 in other systems. In gastric cancer, ALKBH5 stabilizes TXNDC5 mRNA through m6A demethylation to promote malignant progression[12]; in pancreatic neuroendocrine tumors, ALKBH5 increases FABP5 stability in an m6A-IGF2BP2-dependent manner[13]. This study extends this regulatory paradigm to breast cancer, and the identification of the target gene SLC12A8 provides a new molecular explanation for understanding the tumor-promoting mechanism of ALKBH5 in breast cancer. It should be noted that the role of ALKBH5 in breast cancer exhibits significant context dependency[14]. A study by Woodcock et al. [15] based on a large clinical cohort (n=1327) showed that low ALKBH5 protein expression is associated with adverse clinical parameters; Han et al. [16] reported that PRMT6-mediated arginine methylation of ALKBH5 promotes breast cancer tumor growth and glycolytic reprogramming; Zhang et al. [17] found that ALKBH5 was upregulated and inhibited malignant breast cancer phenotypes following BRD4 inhibition. These seemingly contradictory results actually reflect the complexity of ALKBH5 function, which is regulated by multiple post-translational modifications and interacting proteins. This study focuses on the role of the ALKBH5-SLC12A8 axis in a specific therapeutic context (TAM resistance), which is not contradictory to the above studies, but rather supplements the functional dimension of ALKBH5 in breast cancer endocrine therapy resistance.

Furthermore, through GSVA screening and WB validation, we found that the function of SLC12A8 is closely related to the PI3K/AKT/mTOR pathway[18]. After silencing ALKBH5, the expression levels of P-AKT and P-mTOR decreased, directly supporting SLC12A8 as an upstream effector molecule for the activation of this pathway, and also revealing that SLC12A8 may be a key upstream node through which ALKBH5 regulates the PI3K/AKT/mTOR pathway in breast cancer. Previous studies have confirmed that ALKBH5 can activate the PI3K/AKT/mTOR pathway through various downstream targets: in gastric cancer, ALKBH5 inhibits the PI3K/Akt/mTOR cascade through the WRAP53-RALBP1 axis; in pancreatic neuroendocrine tumors, ALKBH5 activates this pathway through FABP5; in age-related macular degeneration, ALKBH5 targets PIK3C2B to regulate AKT/mTOR. However, this study is primarily based on cell models and limited clinical database analysis, and the validation of the ALKBH5-SLC12A8 axis in in vivo models needs to be strengthened. Secondly, the specific molecular mechanism by which SLC12A8 regulates the PI3K/AKT/mTOR pathway—whether it is metabolic reprogramming caused by its NMN transport function or direct activation of the signaling cascade through protein-protein interactions—remains unclear. At the clinical level, it is necessary to verify the correlation between SLC12A8 expression and TAM resistance in a larger cohort of ER-positive breast cancer and to explore the feasibility of using it as a biomarker for predicting resistance.

In summary, this study reveals a novel mechanism by which ALKBH5 stabilizes SLC12A8 mRNA through m6A demethylation, thereby activating the PI3K/AKT/mTOR pathway and promoting TAM resistance in ER-positive breast cancer, providing potential molecular targets and a theoretical basis for overcoming endocrine therapy resistance.

# Declarations

## Ethical Approval and Consent to participate

Not applicable.

**Consent for publication**

Not applicable.

**Availability of supporting data**

The publicly available datasets analysed during the current study were obtained from the TCGA and GTEx databases via the UCSC XENA platform (https://xenabrowser.net/), GEPIA (http://gepia.cancer-pku.cn/), the Kaplan-Meier Plotter (https://kmplot.com/analysis/), SRAMP (http://www.cuilab.cn/sramp/), RM2Target (http://rm2target.canceromics.org/), the GDSC2 database (https://www.cancerrxgene.org/) and the MsigDB database (https://www.gsea-msigdb.org/gsea/msigdb/). The raw experimental data generated in this study (e.g., original western blot and qPCR data) are stored in the laboratory of the corresponding author and are available from the corresponding author upon reasonable request.

**Acknowledgements**

The authors are grateful for the financial support from the funding agencies listed in the Funding section, the public databases and online analysis platforms (TCGA, GTEx, GEPIA, Kaplan-Meier Plotter, SRAMP, RM2Target, GDSC2 and MsigDB) for making their data freely available, and colleagues in our laboratory for their technical assistance and valuable discussions.

## Declaration of Interest Statement

The authors report no conflicts of interest.

Author Contributions

Dongmin Yu: resources, methodology, funding acquisition, writing—review and editing..

Haiyang Guan: investigation, formal analysis,writing-original draft..

Yan Meng:investigation, formal analysis,resources.

Yongzhen Li:visualization,formal analysis.

Haiyan Wang: methodology, writing—review and editing.

Yao Zhou: data curation, formal analysis, project administration.

Rongzhen xie: data curation, resources, writing-review and editing.

All authors have read and agreed to the published version of the manuscript.

Funding

This work is supported by the National Natural Science Foundation of China (Grant No. 82460495), Jiangxi Provincial Natural Science Foundation (20242BAB25353), Jiangxi Provincial Health Commission Science and Technology Plan Project (SKJP220225453) and Ganzhou 2023 Joint "Science & Technology + Medical" Program(2023LNS36669).

**References**

1. Tang Z, Li C, Kang B, Gao G, Li C, Zhang Z. GEPIA: a web server for cancer and normal gene expression profiling and interactive analyses. Nucleic Acids Res. 2017;45(W1):W98-W102. https://doi.org/10.1093/nar/gkx247

2. Győrffy B. Integrated analysis of public datasets for the discovery and validation of survival-associated genes in solid tumors. Innovation (Camb). 2024;5(3):100625. https://doi.org/10.1016/j.xinn.2024.100625

3. Fan R, Cui C, Kang B, Chang Z, Wang G, Cui Q. A combined deep learning framework for mammalian m6A site prediction. Cell Genom. 2024;4(12):100697. https://doi.org/10.1016/j.xgen.2024.100697

4. Kang YJ, Pan L, Liu Y, Rong Z, Liu J, Liu F. GEPIA3: Enhanced drug sensitivity and interaction network analysis for cancer research. Nucleic Acids Res. 2025;53(W1):W283-W290. https://doi.org/10.1093/nar/gkaf423

5. Grozio A, Mills KF, Yoshino J, Bruzzone S, Sociali G, Tokizawa K, et al. Slc12a8 is a nicotinamide mononucleotide transporter. Nat Metab. 2019;1(1):47-57. https://doi.org/10.1038/s42255-018-0009-4

6. Covarrubias AJ, Perrone R, Grozio A, Verdin E. NAD+ metabolism and its roles in cellular processes during ageing. Nat Rev Mol Cell Biol. 2021;22(2):119-141. https://doi.org/10.1038/s41580-020-00313-x

7. Yu D, Ma H, Li D, Tang H, Li W, Li M. Identification of SLC12A8 as a valuable prognostic biomarker and immunotherapeutic target by comprehensive pan-cancer analysis. Gene. 2024;903:148211.

8. Li L, Xia J, Cui R, Kong B. Solute carrier family 12 member 8 impacts the biological behaviors of breast carcinoma cells by activating TLR/NLR signaling pathway. Cytotechnology. 2021;73(1):23-34.

9. Kim JE, Choi J, Park JY, Kim SW, Song N, Shin A, et al. Associations between genetic polymorphisms of membrane transporter genes and prognosis after chemotherapy: meta-analysis and finding from Seoul Breast Cancer Study (SEBCS). Pharmacogenomics J. 2018;18(5):633-645.

10. Garcia-Martinez L, Zhang Y, Nakata Y, Chan HL, Morey L. Epigenetic mechanisms in breast cancer therapy and resistance. Nat Commun. 2021;12(1):1786. https://doi.org/10.1038/s41467-021-22024-3

11. Fang K, Ohihoin AG, Liu T, Yao H, Yang J, Wu J, et al. Integrated single-cell analysis reveals distinct epigenetic-regulated cancer cell states and a heterogeneity-guided core signature in tamoxifen-resistant breast cancer. Genome Med. 2024;16(1):134. https://doi.org/10.1186/s13073-024-01407-3

12. Peng W, Wei X, Zhou F, Xu H. ALKBH5-mediated m6A demethylation of TXNDC5 drives malignant progression in gastric cancer. Epigenomics. 2026;18(1):15-26.

13. Chen J, Ye M, Bai J, He Z, Wang X, Chen Y, et al. ALKBH5 enhances lipid metabolism reprogramming by increasing stability of FABP5 to promote pancreatic neuroendocrine neoplasms progression in an m6A-IGF2BP2-dependent manner. J Transl Med. 2023;21(1):741.

14. Liu X, Li P, Huang Y, Liu Y, Zhang Z, Wang T, et al. M6A demethylase ALKBH5 regulates FOXO1 mRNA stability and chemoresistance in triple-negative breast cancer. Redox Biol. 2024;69:102993. https://doi.org/10.1016/j.redox.2023.102993

15. Woodcock CL, Alsaleem M, Toss MS, Green AR, Rakha EA, Ellis IO. The role of the ALKBH5 RNA demethylase in invasive breast cancer. Discov Oncol. 2024;15(1):343.

16. Han X, Ren C, Jiang A, Hu J, Sun W, Wang D, et al. Arginine methylation of ALKBH5 by PRMT6 promotes breast tumorigenesis via LDHA-mediated glycolysis. Front Med. 2024;18(2):344-356.

17. Zhang H, Lu L, Yi C, Chen S, Yang H, Fan X, et al. BRD4 regulates m6A of ESPL1 mRNA via interaction with ALKBH5 to modulate breast cancer progression. Acta Pharm Sin B. 2025;15(3):1552-1570.

18. Nunnery SE, Mayer IA. Targeting the PI3K/AKT/mTOR Pathway in Hormone-Positive Breast Cancer. Drugs. 2020;80(16):1685-1697. https://doi.org/10.1007/s40265-020-01394-w

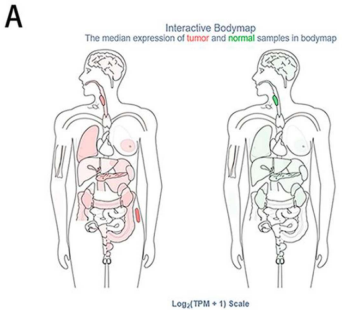
A
Interactive Bodymap
The median expression of tumor and normal samples in bodymap
Log2(TPM + 1) Scale

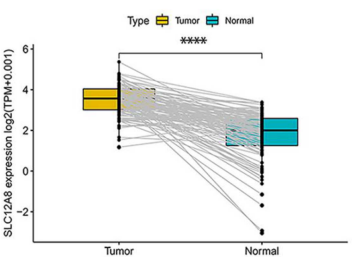
B
Type Tumor Normal
****
SLC12A8 expression log2(TPM+0.001)
Tumor
Normal
BRCA

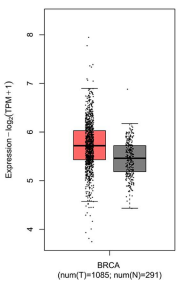
C
Expression ~ log2(TPM+1)
BRCA
(num(T)=1085; num(N)=291)

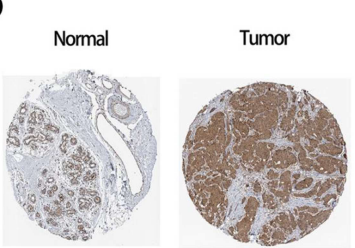
D
Normal
Tumor

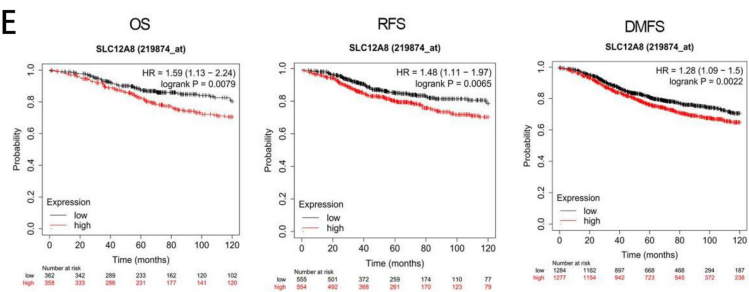
E
OS
SLC12A8 (219874_at)
HR = 1.59 (1.13 − 2.24)
logrank P = 0.0079
RFS
SLC12A8 (219874_at)
HR = 1.48 (1.11 − 1.97)
logrank P = 0.0065
DMFS
SLC12A8 (219874_at)
HR = 1.28 (1.09 − 1.5)
logrank P = 0.0022
Probability
Time (months)
Expression
low
high
Number at risk

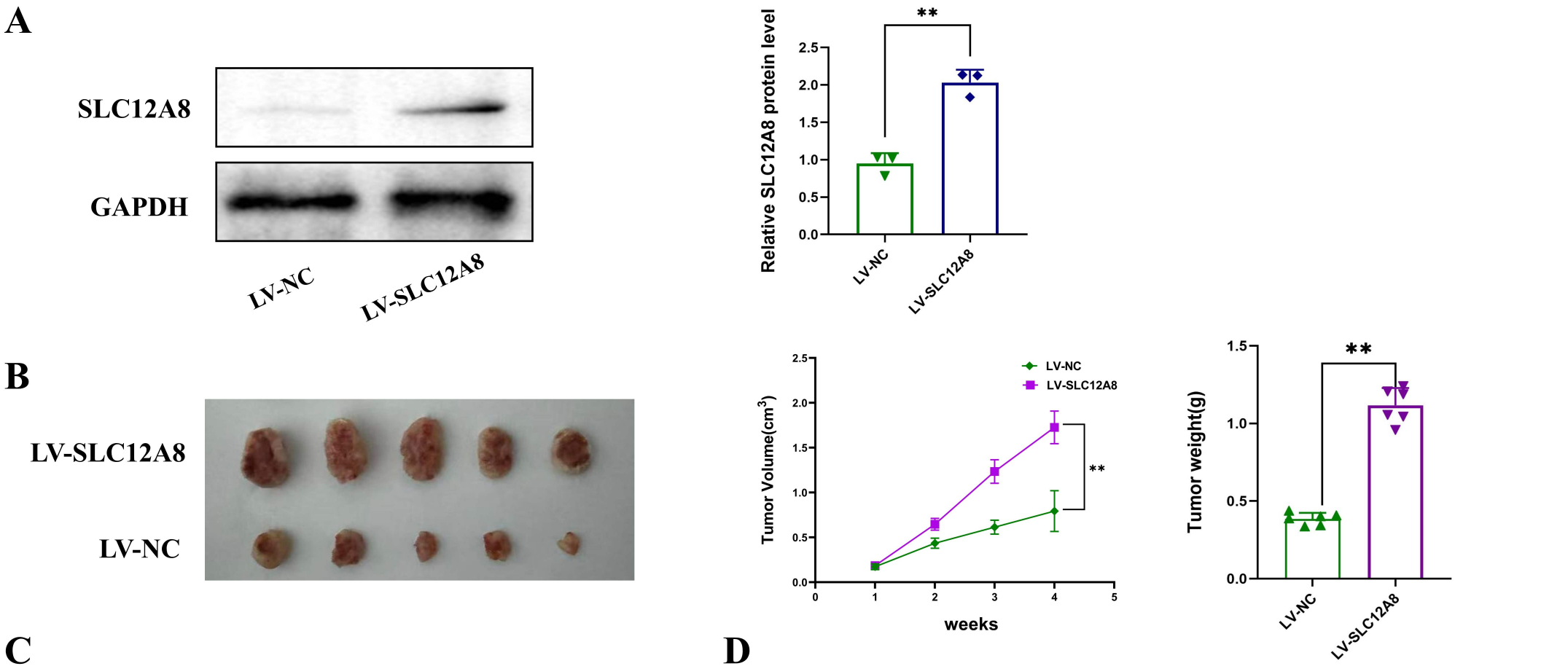
A
SLC12A8
GAPDH
LV-NC
LV-SLC12A8
Relative SLC12A8 protein level
**
2.5
2.0
1.5
1.0
0.5
0.0
LV-NC
LV-SLC12A8
B
LV-SLC12A8
LV-NC
Tumor Volume(cm3)
LV-NC
LV-SLC12A8
**
weeks
Tumor weight(g)
**
C
LV-NC
LV-SLC12A8
D
LV-NC
LV-SLC12A8

A

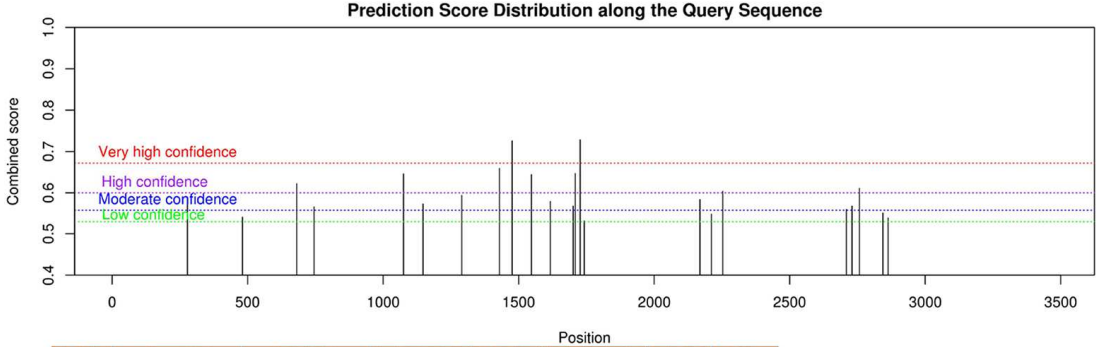


B

| # | Position | Sequence context | Structural context | Local structure visualization | Score(binary) | Score(knn) | Score(spectrum) | Score(combined) | Decision |
|---|---|---|---|---|---|---|---|---|---|
| 1 | 234 | UGGGG UUGUG CUCUU<br>CCUGA GGACU GGCUG<br>GCUGG UGGGA AACAC | N/A | N/A | 0.699 | 0.528 | 0.428 | 0.582 | m$^6$A site (Moderate confidence) |
| 2 | 437 | UCGGG CUGCU CUAUG<br>UGUUU GGACA GUGUG<br>UUGCA GGUGC CAUGU | N/A | N/A | 0.589 | 0.594 | 0.466 | 0.540 | m$^6$A site (Low confidence) |
| 3 | 637 | CUGCU GGCCG UGUCC<br>ACACU GGACU UUGUG<br>GUGGG UUCUU UCACC | N/A | N/A | 0.707 | 0.679 | 0.498 | 0.622 | m$^6$A site (High confidence) |
| 4 | 701 | GUUUC AUUGG AUAUU<br>CACCC GAACU GCUAC<br>AGAAC AACAC GCUGC | N/A | N/A | 0.632 | 0.702 | 0.46 | 0.566 | m$^6$A site (Moderate confidence) |
| 5 | 1031 | CCCUG GCUUC CUGCA<br>UGGGA GGACU UUAUG<br>GAGCU CCCCG CAUCC | N/A | N/A | 0.690 | 0.577 | 0.594 | 0.646 | m$^6$A site (High confidence) |
| 6 | 1103 | UCCCU GCACU UGCCU<br>GUCUG GGACA AGGGA<br>AGGGG CCAAA CAAAA | N/A | N/A | 0.607 | 0.602 | 0.524 | 0.573 | m$^6$A site (Moderate confidence) |
| 7 | 1246 | AUGCU GACAU ACGUU<br>GCAGU GGACU ACUCU<br>UACUU CUCCC UGUCC | N/A | N/A | 0.636 | 0.723 | 0.522 | 0.594 | m$^6$A site (Moderate confidence) |
| 8 | 1385 | CUCCC AGUUA CGGCU<br>CUGAG GGACC UGCCC<br>AAAGA GUCUU GGAGG | N/A | N/A | 0.614 | 0.745 | 0.709 | 0.659 | m$^6$A site (High confidence) |
| 9 | 1432 | ACGCU ACUGG AAUUC<br>ACCAA GGACA UGGAU<br>CAGCU CCUCC AGCUA | N/A | N/A | 0.732 | 0.692 | 0.723 | 0.726 | m$^6$A site (Very high confidence) |
| 10 | 1503 | CAGGC AAGGA GAGGG<br>UAACA GGACC CCAGA<br>AAGUC AGAAG AGGAA | N/A | N/A | 0.585 | 0.701 | 0.718 | 0.644 | m$^6$A site (High confidence) |
| 11 | 1573 | CUACA AGAUA GCUUC<br>CUCUU GGACC UCAAA<br>UCCCC UCCUU CUAUC | N/A | N/A | 0.520 | 0.643 | 0.652 | 0.579 | m$^6$A site (Moderate confidence) |
| 12 | 1657 | GAGGG GCAGG AGUCC<br>UGCUG GAACA AGCAG<br>ACUUC CAAGA GCGAA | N/A | N/A | 0.456 | 0.789 | 0.694 | 0.568 | m$^6$A site (Moderate confidence) |
| 13 | 1665 | GGAGU CCUGC UGGAA<br>CAGGC AGACU UCCAA<br>GAGCG AAGGG ACUCA | N/A | N/A | 0.615 | 0.657 | 0.692 | 0.647 | m$^6$A site (High confidence) |
| 14 | 1683 | GCAGA CUUCC AAGAG<br>CGAAG GGACU CAGCC<br>UGAGG GAACA UAUGG | N/A | N/A | 0.771 | 0.786 | 0.661 | 0.728 | m$^6$A site (Very high confidence) |
| 15 | 1698 | CGAAG GGACU CAGCC<br>UGAGG GAACA UAUGG<br>AGAGC AACUU GUUCC | N/A | N/A | 0.428 | 0.568 | 0.670 | 0.531 | m$^6$A site (Low confidence) |
| 16 | 2125 | CAGCU CACCC AGGAG<br>AAUGC AGACU UCGCC<br>ACUCG GGAUC GCUAC | N/A | N/A | 0.576 | 0.661 | 0.585 | 0.584 | m$^6$A site (Moderate confidence) |
| 17 | 2167 | UACCA CCACU CCUCC<br>CUCGU GAACC GGGAG<br>CAGCU GAUGC CUCAC | N/A | N/A | 0.447 | 0.737 | 0.661 | 0.547 | m$^6$A site (Low confidence) |
| 18 | 2209 | CACUA CUAGA UGCAG<br>UGCUG GGACC UUCCU<br>CUUUU GGAGC UGUCC | N/A | N/A | 0.514 | 0.704 | 0.715 | 0.604 | m$^6$A site (High confidence) |
| 19 | 2665 | CAGAA AUCUA UGUUU<br>UCUUA GAACA UGUGG<br>AAGAA GGAAA AAGAC | N/A | N/A | 0.48 | 0.428 | 0.688 | 0.560 | m$^6$A site (Moderate confidence) |
| 20 | 2686 | AACAU GUGGA AGAAG<br>GAAAA AGACA AAAAA<br>GGAAA UCUGG AUUCU | N/A | N/A | 0.480 | 0.443 | 0.704 | 0.568 | m$^6$A site (Moderate confidence) |
| 21 | 2713 | AAAGG AAAUC UGGAU<br>UCUGA GGACC ACGUC<br>UCACC CAGGG UGACA | N/A | N/A | 0.543 | 0.628 | 0.701 | 0.611 | m$^6$A site (High confidence) |
| 22 | 2800 | AGAGC UCUAU ACAGG<br>UACUA AGACU AGCAG<br>GGGAC ACCAA GACUC | N/A | N/A | 0.573 | 0.366 | 0.540 | 0.550 | m$^6$A site (Low confidence) |
| 23 | 2819 | AAGAC UAGCA GGGGA<br>CACCA AGACU CUGCA<br>CAACC AGAUU GCUUG | N/A | N/A | 0.635 | 0.496 | 0.459 | 0.557 | m$^6$A site (Low confidence) |

C

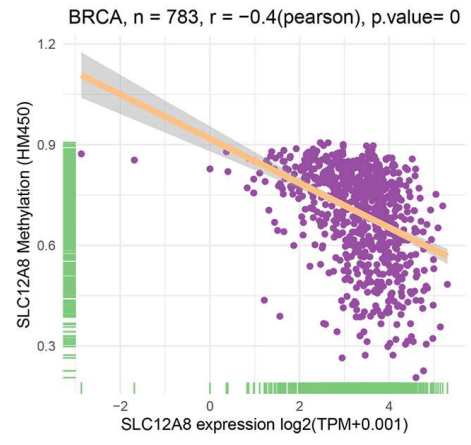


D

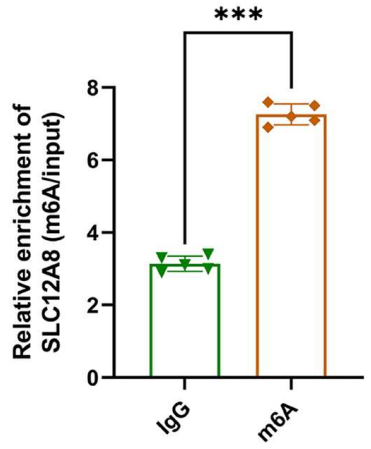


E

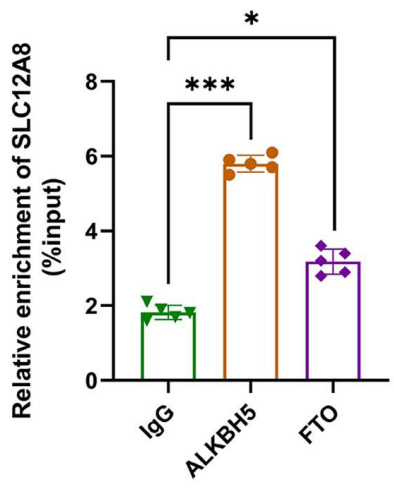

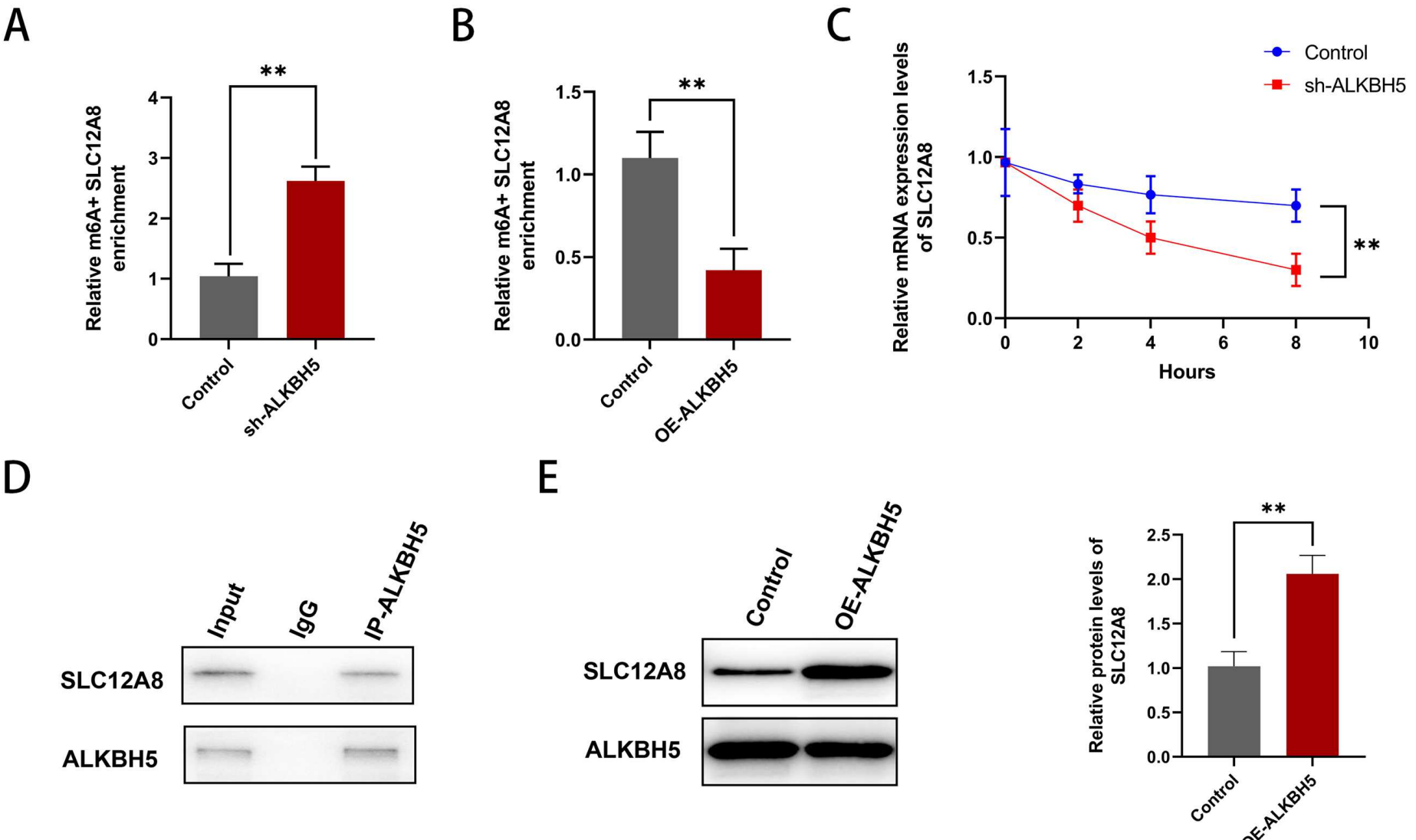
A
Relative m6A+ SLC12A8 enrichment
**
Control
sh-ALKBH5
B
Relative m6A+ SLC12A8 enrichment
**
Control
OE-ALKBH5
C
Relative mRNA expression levels of SLC12A8
Control
sh-ALKBH5
**
Hours
D
Input
IgG
IP-ALKBH5
SLC12A8
ALKBH5
E
Control
OE-ALKBH5
SLC12A8
ALKBH5
Relative protein levels of SLC12A8
**
Control
OE-ALKBH5

A

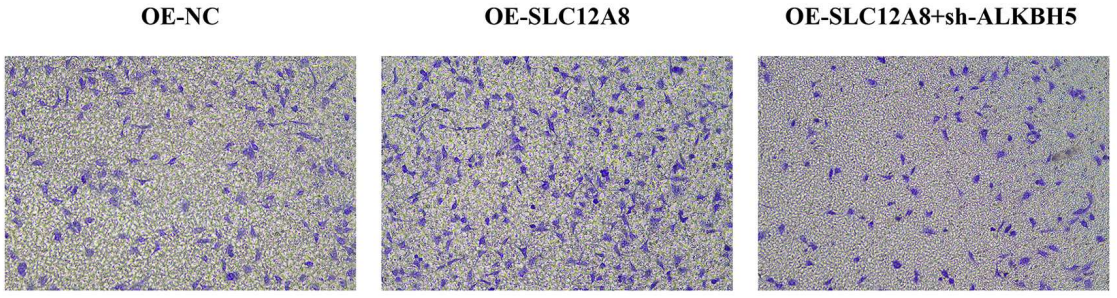
OE-NC
OE-SLC12A8
OE-SLC12A8+sh-ALKBH5

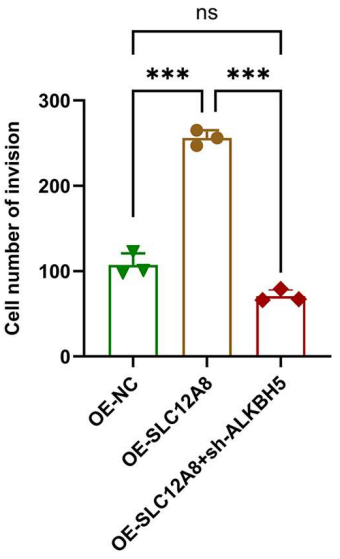
ns
***
***
300
200
100
0
Cell number of invision
OE-NC
OE-SLC12A8
OE-SLC12A8+sh-ALKBH5

B

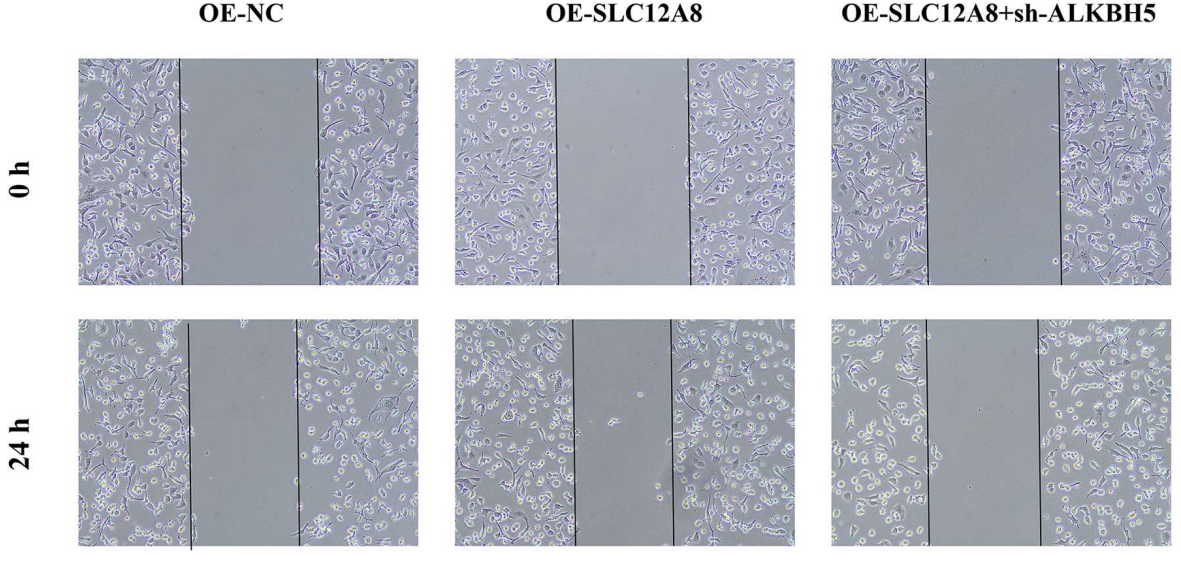
OE-NC
OE-SLC12A8
OE-SLC12A8+sh-ALKBH5
0 h
24 h

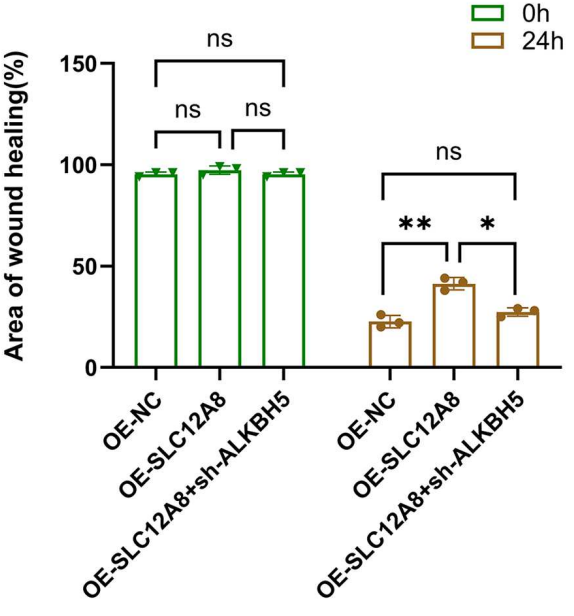
0h
24h
ns
ns
ns
ns
**
*
150
100
50
0
Area of wound healing(%)
OE-NC
OE-SLC12A8
OE-SLC12A8+sh-ALKBH5
OE-NC
OE-SLC12A8
OE-SLC12A8+sh-ALKBH5

A

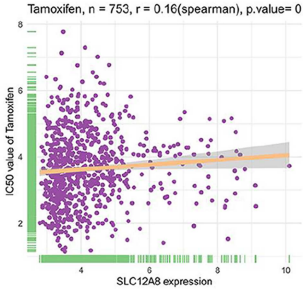
Tamoxifen, n = 753, r = 0.16(spearman), p.value= 0
IC50 value of Tamoxifen
SLC12A8 expression

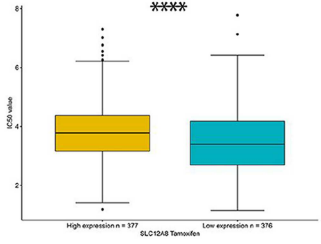
****
IC50 value
High expression n = 377
Low expression n = 376
SLC12A8 Tamoxifen

B

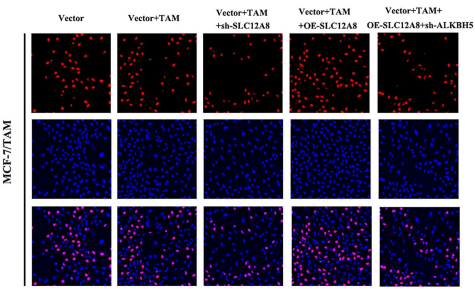
Vector
Vector+TAM
Vector+TAM +sh-SLC12A8
Vector+TAM +OE-SLC12A8
Vector+TAM+ OE-SLC12A8+sh-ALKBH5
MCF-7/TAM

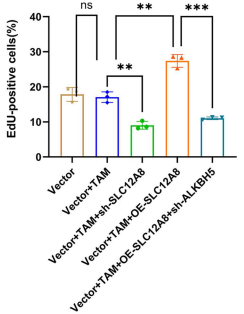
EdU-positive cells(%)
ns
**
***
**
Vector
Vector+TAM
Vector+TAM+sh-SLC12A8
Vector+TAM+OE-SLC12A8
Vector+TAM+OE-SLC12A8+sh-ALKBH5

C

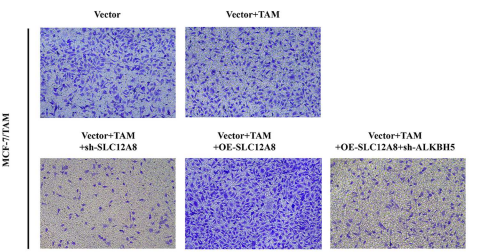
Vector
Vector+TAM
Vector+TAM +sh-SLC12A8
Vector+TAM +OE-SLC12A8
Vector+TAM +OE-SLC12A8+sh-ALKBH5
MCF-7/TAM

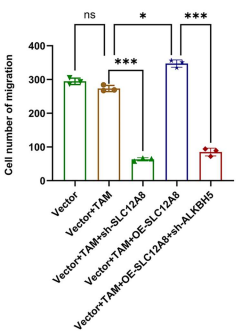
Cell number of migration
ns
*
***
***
Vector
Vector+TAM
Vector+TAM+sh-SLC12A8
Vector+TAM+OE-SLC12A8
Vector+TAM+OE-SLC12A8+sh-ALKBH5

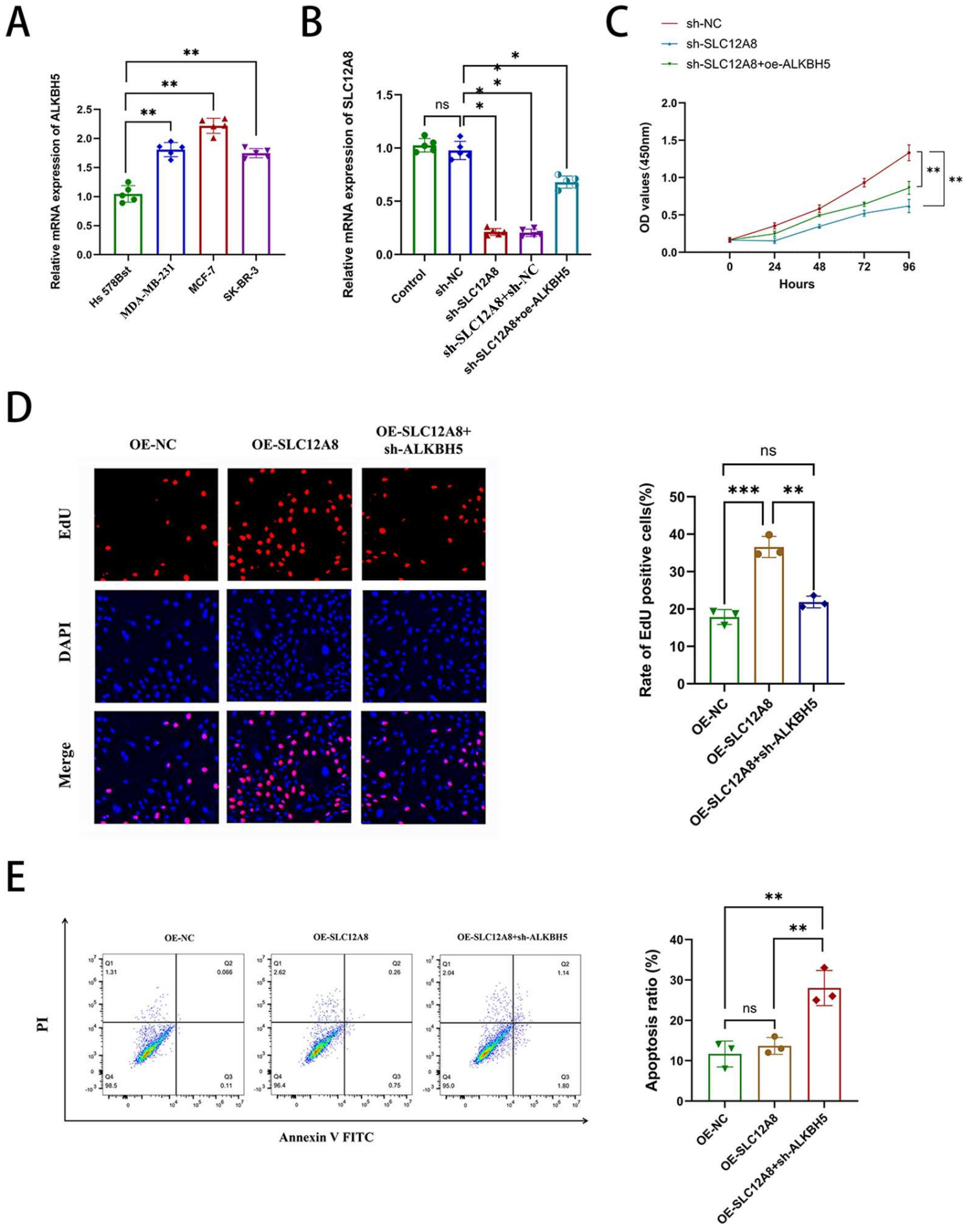
A
Relative mRNA expression of ALKBH5
Hs 578Bst
MDA-MB-231
MCF-7
SK-BR-3
B
Relative mRNA expression of SLC12A8
ns
Control
sh-NC
sh-SLC12A8
sh-SLC12A8+sh-NC
sh-SLC12A8+oe-ALKBH5
C
sh-NC
sh-SLC12A8
sh-SLC12A8+oe-ALKBH5
OD values (450nm)
Hours
D
OE-NC
OE-SLC12A8
OE-SLC12A8+ sh-ALKBH5
EdU
DAPI
Merge
Rate of EdU positive cells(%)
E
OE-NC
OE-SLC12A8
OE-SLC12A8+sh-ALKBH5
PI
Annexin V FITC
Apoptosis ratio (%)

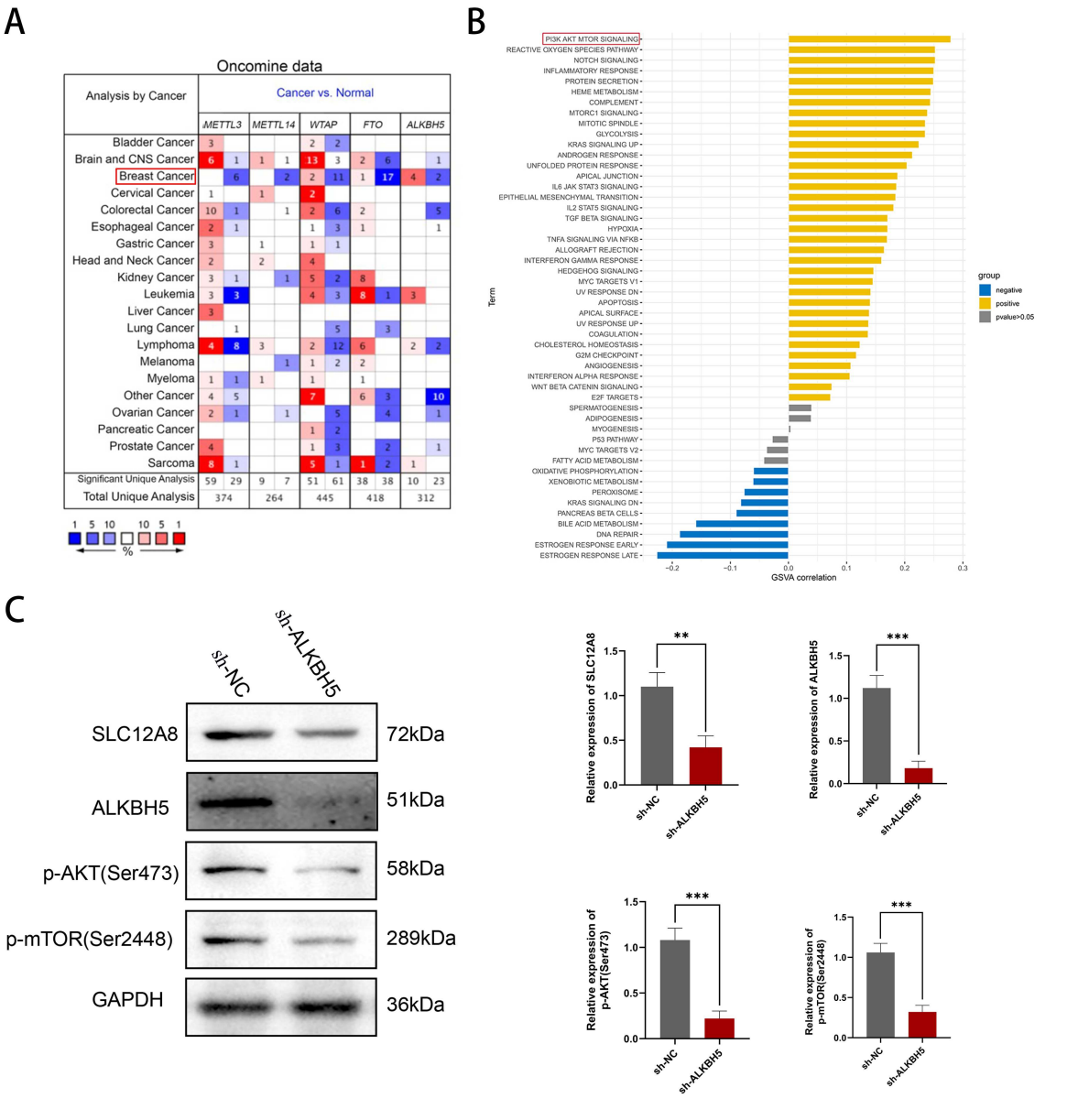
A
Oncomine data
Analysis by Cancer
Cancer vs. Normal
METTL3
METTL14
WTAP
FTO
ALKBH5
Bladder Cancer
Brain and CNS Cancer
Breast Cancer
Cervical Cancer
Colorectal Cancer
Esophageal Cancer
Gastric Cancer
Head and Neck Cancer
Kidney Cancer
Leukemia
Liver Cancer
Lung Cancer
Lymphoma
Melanoma
Myeloma
Other Cancer
Ovarian Cancer
Pancreatic Cancer
Prostate Cancer
Sarcoma
Significant Unique Analysis
Total Unique Analysis
1 5 10 10 5 1
%
B
PI3K AKT MTOR SIGNALING
REACTIVE OXYGEN SPECIES PATHWAY
NOTCH SIGNALING
INFLAMMATORY RESPONSE
PROTEIN SECRETION
HEME METABOLISM
COMPLEMENT
MTORC1 SIGNALING
MITOTIC SPINDLE
GLYCOLYSIS
KRAS SIGNALING UP
ANDROGEN RESPONSE
UNFOLDED PROTEIN RESPONSE
APICAL JUNCTION
IL6 JAK STAT3 SIGNALING
EPITHELIAL MESENCHYMAL TRANSITION
IL2 STAT5 SIGNALING
TGF BETA SIGNALING
HYPOXIA
TNFA SIGNALING VIA NFKB
ALLOGRAFT REJECTION
INTERFERON GAMMA RESPONSE
HEDGEHOG SIGNALING
MYC TARGETS V1
UV RESPONSE DN
APOPTOSIS
APICAL SURFACE
UV RESPONSE UP
COAGULATION
CHOLESTEROL HOMEOSTASIS
G2M CHECKPOINT
ANGIOGENESIS
INTERFERON ALPHA RESPONSE
WNT BETA CATENIN SIGNALING
E2F TARGETS
SPERMATOGENESIS
ADIPOGENESIS
MYOGENESIS
P53 PATHWAY
MYC TARGETS V2
FATTY ACID METABOLISM
OXIDATIVE PHOSPHORYLATION
XENOBIOTIC METABOLISM
PEROXISOME
KRAS SIGNALING DN
PANCREAS BETA CELLS
BILE ACID METABOLISM
DNA REPAIR
ESTROGEN RESPONSE EARLY
ESTROGEN RESPONSE LATE
Term
GSVA correlation
group
negative
positive
pvalue>0.05
C
sh-NC
sh-ALKBH5
SLC12A8
ALKBH5
p-AKT(Ser473)
p-mTOR(Ser2448)
GAPDH
72kDa
51kDa
58kDa
289kDa
36kDa
Relative expression of SLC12A8
Relative expression of ALKBH5
Relative expression of p-AKT(Ser473)
Relative expression of p-mTOR(Ser2448)

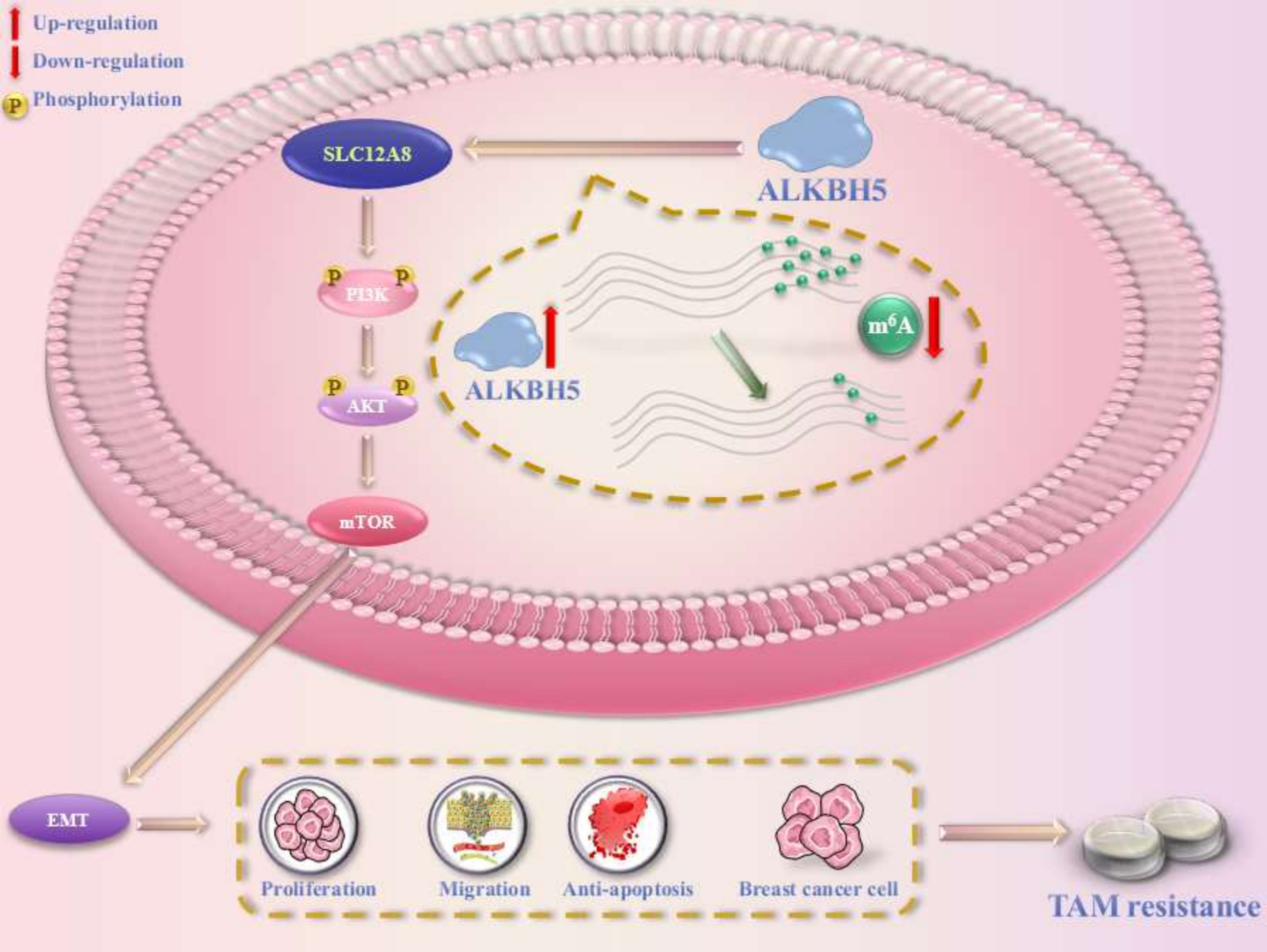
Up-regulation
Down-regulation
Phosphorylation
SLC12A8
ALKBH5
PI3K
AKT
mTOR
ALKBH5
m6A
EMT
Proliferation
Migration
Anti-apoptosis
Breast cancer cell
TAM resistance

## Supplementary Files

This is a list of supplementary files associated with this preprint. Click to download.

- fig8CALKBH5.tif
- fig8CGAPDH.tif
- fig8CpAKTSer473.tif
- fig8CpmTORSer2448.tif
- fig8CSLC12A8.tif
- fig2gapdh.jpg
- fig2SLC12A8.tif
- fig4eALKBH5.jpg
- fig4DALKBH5.tif
- fig4DSLC12A8.tif
- fig4eSLC12A8.tif